Slowing light in $\chi^{(2)}$ photonic crystals

G. D'Aguanno,[1,2,*] M. Centini,[1,2] M. Scalora,[2] C. Sibilia,[1] M. Bertolotti,[1] E. Fazio,[1] C. M. Bowden,[2] and M. J. Bloemer[2]
[1]*INFM at Dipartimento di Energetica, Università di Roma "La Sapienza," Via A. Scarpa 16, I-00161 Rome, Italy*
[2]*Weapons Sciences Directorate, Research Development and Engineering Center, U.S. Army Aviation & Missile Command, Building 7804, Redstone Arsenal, Alabama 35898-5000, USA*
(Received 11 September 2002; revised manuscript received 7 August 2003; published 28 October 2003)

A study of parametric nonlinear frequency down-conversion in photonic crystals reveals that under suitable conditions the probe field can be slowed down to approximately 11 m/s. The effect arises as a result of the simultaneous availability of global phase-matching conditions, field localization, and gain experienced by the probe beam. Together, these effects conspire to yield tunneling velocities previously reported only for coherently resonant interactions, i.e., electromagnetic induced transparency, in Bose-Einstein condensates, hot atomic gases, and doped crystals.

DOI: 10.1103/PhysRevE.68.046613 PACS number(s): 42.70.Qs, 42.65.Ky, 42.65.Yj

Recent experiments have shown the reduction of the group velocity of light pulses to 17 m/s in a Bose condensate of ultracold sodium atoms [1], 90 m/s in a hot rubidium gas [2], and 45 m/s in a Pr-doped Y_2SiO_5 crystal [3]. The effect is often referred to as light trapping, and it involves a resonant interaction between a control and a signal beam, tuned such that quantum coherence is established between an excited state and two nearly degenerate ground states [1–3]. The signal beam experiences an effective dispersion such that its group velocity becomes a minimum in a region of transparency [electromagnetically induced transparency (EIT)].

In this article we show that light may also be slowed down to velocities of only a few meters per second as a result of a parametric down-conversion process in a one-dimensional (1D) photonic crystal (PC). Rather than relying on quantum mechanical interactions between atomic levels resonant with the incident light, the phenomenon we describe occurs as a result of the geometrical confinement of light within a structure of finite length followed by the onset of nonlinear gain. This process therefore begins purely as an interferometric phenomenon that manifests itself initially with the creation of classical Fabry-Pérot-like transmission resonances [see inset (b) of Fig. 1]. Then we allow two quasimonochromatic beams (or pulses whose frequency bandwidth is much narrower than the resonance bandwidth), a weak fundamental frequency (FF), and a much more intense second harmonic (SH) field, to enter a $\chi^{(2)}$ PC. Finally, we take advantage of the enhancement of quadratic interactions due to the simultaneous availability of high field localization and robust, exact phase-matching conditions [4,5] to amplify the FF. As a result, the FF pulse can slow down to just a few meters per second.

To illustrate the dynamics just described, we write the coupled mode equations that govern the interaction of two linearly polarized, quasimonochromatic waves, one tuned at the FF ω, and the other tuned at the SH frequency 2ω, in a 1D finite structure [6,7]:

$$\sum_{l=+,-} p_{\omega}^{(+,l)} \frac{dA_{\omega}^{(l)}}{dz} = i\frac{\omega}{c} \sum_{(k,l)=(+,-)} \Gamma_{(\omega,+)}^{(k,l)} A_{2\omega}^{(k)} A_{\omega}^{(l)*}, \quad (1a)$$

$$\sum_{l=+,-} p_{\omega}^{(-,l)} \frac{dA_{\omega}^{(l)}}{dz} = i\frac{\omega}{c} \sum_{(k,l)=(+,-)} \Gamma_{(\omega,-)}^{(k,l)} A_{2\omega}^{(k)} A_{\omega}^{(l)*}, \quad (1b)$$

$$\sum_{l=+,-} p_{2\omega}^{(+,l)} \frac{dA_{2\omega}^{(l)}}{dz} = i\frac{\omega}{c} \sum_{(k,l)=(+,-)} \Gamma_{(2\omega,+)}^{(k,l)} A_{\omega}^{(k)} A_{\omega}^{(l)}, \quad (1c)$$

$$\sum_{l=+,-} p_{2\omega}^{(-,l)} \frac{dA_{2\omega}^{(l)}}{dz} = i\frac{\omega}{c} \sum_{(k,l)=(+,-)} \Gamma_{(2\omega,-)}^{(k,l)} A_{\omega}^{(k)} A_{\omega}^{(l)}, \quad (1d)$$

where $p_{j\omega}^{(k,l)} = \langle \Phi_{j\omega}^{(k)} | \hat{p}_{j\omega} \Phi_{j\omega}^{(l)} \rangle$ for $j=1,2$ and $k,l=+,-$, $\Gamma_{(\omega,n)}^{(k,l)} = \langle \Phi_{\omega}^{(n)} | d^{(2)} \Phi_{2\omega}^{(k)} \Phi_{\omega}^{(l)*} \rangle$, $\Gamma_{(2\omega,n)}^{(k,l)} = \langle \Phi_{2\omega}^{(n)} | d^{(2)} \Phi_{\omega}^{(k)} \Phi_{\omega}^{(l)} \rangle$ for $n,k,l=+,-$. The solutions for the electric fields can be expressed as follows: $E_{j\omega} = A_{j\omega}^{(+)}(z)\Phi_{j\omega}^{(+)}(z) + A_{j\omega}^{(-)}(z)\Phi_{j\omega}^{(-)}(z)$, where $A_{j\omega}^{(\pm)}$ are the complex amplitudes of the electric field. Equations (1) can be derived from a first order multiple scale expansion performed on the nonlinear Helmholtz equations [6,7]. The reader interested in the details of the derivation can consult Ref. [6]. $\{\Phi_{j\omega}^{(\pm)}\}$ are the left-to-right (LTR, $+$) and right-to-left (RTL, $-$) linear modes, which can be calculated independently using the standard linear matrix-transfer technique, assuming a zero nonlinear coupling coefficient and an electric field of unitary amplitude incident from either the left (LTR) or the right (RTL) side of the stack. The $p_{j\omega}^{(k,l)}$ are the matrix elements of the momentum operator $\hat{p}_{j\omega} \equiv -i(c/j\omega)d/dz$, calculated over the LTR and RTL modes using the standard metric $\langle f|g\rangle \equiv (1/L)\int_0^L f^*(z)g(z)dz$. $d^{(2)}(z)$ is a spatially dependent, quadratic coupling function, and $\Gamma_{(j\omega,n)}^{(k,l)}$ are overlap integrals.

As a first example, we consider a 1D PC whose details are given in the caption of Fig. 1. Layer thicknesses and materials can be chosen such that the FF field is tuned to the first transmission resonance near the first order band gap, and the

*Electronic address: giuseppe.daguanno@uniroma1.it

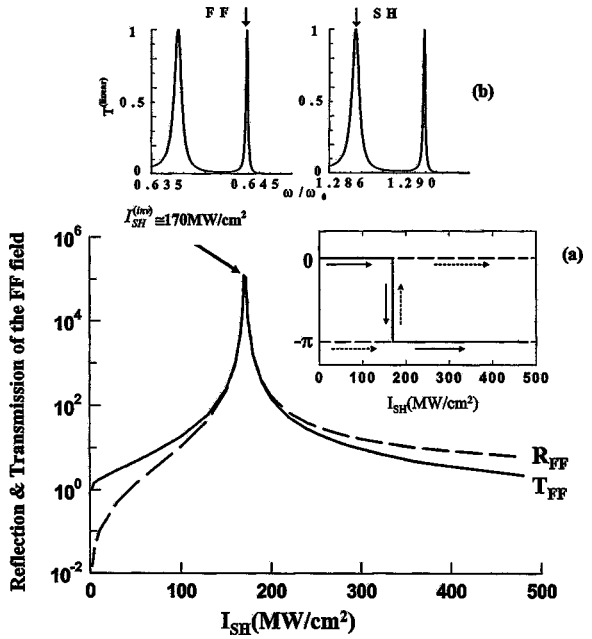

FIG. 1. $R_{\mathrm{FF}}=|A_\omega^{(-)}(0)|^2/|A_\omega^{(+)}(0)|^2$ (dashed line) and $T_{\mathrm{FF}}=|A_\omega^{(+)}(L)|^2/|A_\omega^{(+)}(0)|^2$ (solid line) vs SH input intensity. The arrow indicates the SH input intensity that leads to the inversion of the process. (a) Phase of the FF field upon reflection, $\phi_r=\arg[A_\omega^{(-)}(0)/A_\omega^{(+)}(0)]$ (dashed line) and upon transmission $\phi_t=\arg[A_\omega^{(+)}(L)/A_\omega^{(+)}(0)]$ (solid line) vs SH input intensity. (b) Linear transmittance vs normalized frequency ω/ω_0, $\omega_0=2\pi c/\lambda_0$, $\lambda_0=1\ \mu$m for a structure of total length $L=7.11\ \mu$m composed of 59 alternating layers of 90 nm of air ($n_L=1$) and 150 nm of a quadratic dielectric material ($d^{(2)}=120$ pm/V) whose indexes of refraction at the FF ($\lambda=1.55\ \mu$m) and SH frequency are, respectively, $n_H(\omega)=3.342$ and $n_H(2\omega)=3.61$. The arrows identify tuning of the FF and SH fields, respectively. The spectral bandwidth of the FF transmission resonance is $\Delta\omega\approx 10^3$ GHz, which corresponds to a lifetime of approximately 5 ps.

SH field is tuned to the second transmission resonance near the second order band gap, as shown in inset (b) of Fig. 1. Tuning in this fashion causes the SH field to be globally phase matched with the FF field [4,5], leading to enhanced second harmonic generation (SHG) [5,6].

We numerically integrated Eqs. (2) using a shooting procedure [8]. When both the input FF and SH fields are present, the efficiency of the interaction depends on the relative phase difference $\delta\phi$ between the input fields. In particular, the FF transmitted and reflected components undergo an amplification process that is enhanced for $\delta\phi=3\pi/4+m\pi$, while deamplification takes place if $\delta\phi=\pi/4+m\pi$ ($m=0,1,2...$). We choose the condition of maximum amplification for the FF field, $\delta\phi=3\pi/4$, take the SH input intensity I_{SH} in the range 2–500 MW/cm^2, and $I_{\mathrm{FF}}=0.1$ W/cm^2. Our calculations show that the SH field always remains undepleted to levels less than 0.1%. In Fig. 1 we show the reflection R_{FF}, the transmission T_{FF}, and the phases of the FF field vs the SH input intensity. The figure shows that the FF field displays a resonancelike dynamics by first increasing sharply by several orders of magnitude as a function of input SH intensity, followed by an equally sharp decrease beginning at about 170 MW/cm^2. The reason for this decline is that a π phase shift has occurred in both reflected and transmitted fields [see inset (a) of Fig. 1], leading to a reversal of energy flow in favor of the SH field.

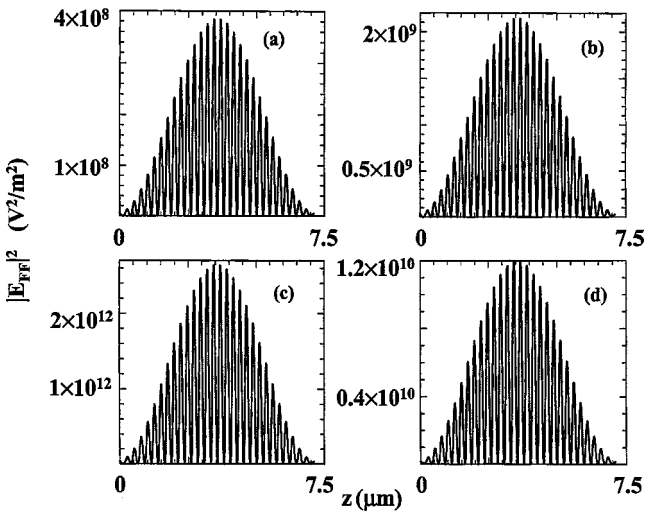

FIG. 2. Absolute value squared of the FF field inside the PBG structure, for different values of the input SH intensity. $I_{\mathrm{SH}}^{(\mathrm{input})}$ = (a) 50, (b) 110, (c) 169, and (d) 200 MW/cm^2.

The sort of dynamics just described, which includes a π phase shift accompanied by the inversion of gain, is typical of bulk $\chi^{(2)}$ materials under exact phase-matching conditions [9]. In our case, however, the unique combination of strong feedback, field localization, robust phase-matching conditions, and gain produces the extreme circumstances that manifest themselves in the remarkable resonancelike behavior shown in Fig. 1, which ultimately do not allow the SH to become depleted. The reflection and the transmission of the FF field reach their maxima ($I^{\mathrm{reflected}}\sim I^{\mathrm{transmitted}}\sim 0.1$ MW/cm^2) at the point of inversion of nonlinear gain when $I_{\mathrm{SH}}^{(\mathrm{inv})}\cong 170$ MW/cm^2. In Fig. 2 we show typical localization properties of the FF field inside the photonic band gap (PBG) structure. The figure suggests that the FF field shape remains the same, an indication that no shifts of the resonances occur, and that the original phase-matching conditions endure. In Fig. 3(a) we show the reflection R_{FF} and the transmission T_{FF}, for the same structure of Fig. 1, but with $d^{(2)}=30$ pm/V. In Fig. 3(b) we present results for a structure similar to that of Fig. 3(a), but instead of air we use a material with $n_L=1.5$.

Several points can now be made with the aid of the figures. (i) A comparison between Figs. 1 and 3(a) shows that the threshold SH input intensity necessary to invert the process scales as $I_{\mathrm{SH}}^{(\mathrm{inv})}\approx(1/d^{(2)})^2$. This scaling law has been tested and holds for other values of $d^{(2)}$. (ii) Comparing Figs. 3(a) and 3(b) reveals that $I_{\mathrm{SH}}^{(\mathrm{inv})}$ is also affected by the index contrast $\delta n=n_H-n_L$: from 2.7 GW/cm^2 in Fig. 3(a) where $\delta n\cong 2.5$ to $I_{\mathrm{SH}}^{(\mathrm{inv})}\cong 5.9$ GW/cm^2 when $\delta n\cong 2$ in Fig. 3(b). Clearly, the index contrast determines initial resonance bandwidth, and therefore it changes the efficiency of the process. (iii) Figs. 1 and 3 show that the dynamics we have described is general, i.e., independent of any particular

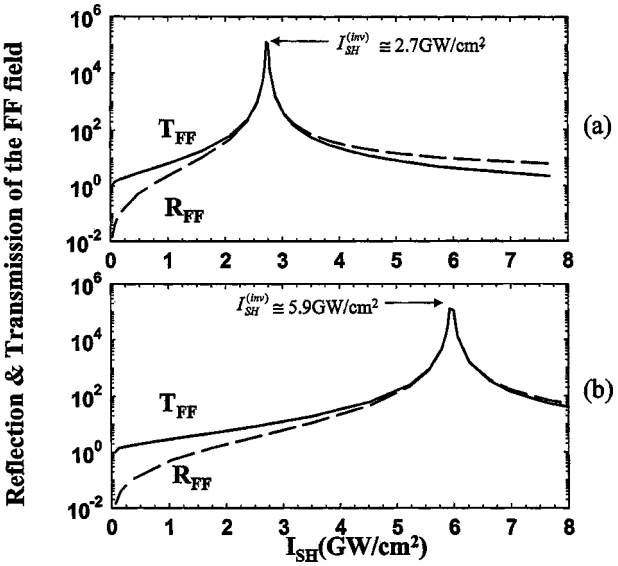

FIG. 3. (a) R_{FF} (dashed line) and T_{FF} (solid line) vs SH input intensity. The structure is the same as that of Fig. 1, but with $d^{(2)}=30$ pm/V. (b) R_{FF} (dashed line) and T_{FF} (solid line) vs SH input intensity. The structure is similar to that of (a), except that the low-index layers have an index $n_L=1.5$. The arrows indicate the SH input intensity that leads to the inversion of the process.

choice of material or nonlinear coefficient. The specific materials one chooses determine a particular $I_{\mathrm{SH}}^{(\mathrm{inv})}$ but leave unaltered the shape of the curves in Figs. 1 and 3. In real structures, absorption and/or scattering losses may also influence the magnitude of $I_{\mathrm{SH}}^{(\mathrm{inv})}$ but will not negate the effect. A detailed discussion of materials suitable for an experimental verification is beyond the scope of this article. Suffice it to say here that structures made of air/semiconductor materials may be obtained by etching GaAs waveguides [10]. Structures similar to the one described in Fig. 3(b), i.e., $Al_2O_3(n\sim 1.5)$/GaAs($n\sim 3.5$), have also been fabricated and tested for SHG under global phase-matching conditions [5] in the undepleted pump regime.

As outlined in Refs. [11,12], the tunneling time of a quasimonochromatic pulse that traverses a finite barrier is directly proportional to the electromagnetic energy density stored within the structure. Figure 2 thus suggests that the tunneling velocity of the FF pulse may be modulated by controlling the SH intensity: the pulse slows down for intensities below $I_{\mathrm{SH}}\sim 170$ MW/cm^2, and it speeds up above this value. The approach followed in Ref. [11] for linear interactions can be generalized to the nonlinear case. We write the expression for the energy velocity $V_{\omega,E}$ of a plane, quasimonochromatic, FF wave of carrier frequency ω that traverses a barrier of length L: $V_{\omega,E}=[\vec{S}_\omega(z=L^+)\cdot\hat{z}]/\langle U_\omega(z)\rangle$, where $\vec{S}_\omega(z=L^+)$ is the time-averaged Poynting vector calculated at the exit surface $z=L^+$, $\hat{z}$ is the unit vector along the propagation direction of the transmitted field, and $U_\omega(z)$ is the time-averaged electromagnetic energy density. $\langle U_\omega(z)\rangle \equiv (1/L)\int_0^L U_\omega(z)dz$ denotes the spatial average of the energy density over the barrier length. Using appropriate boundary conditions, it is straightforward to verify that the quantity $\vec{S}_\omega(z=L^+)\cdot\hat{z}$ can be expressed as a function of the transmission T_{FF} of the barrier and the amplitude $E_\omega^{(\mathrm{input})}$ of the incident FF field in the following way: $\vec{S}_\omega(z=L^+)\cdot\hat{z}=(\varepsilon_0 c/2)|E_\omega^{(\mathrm{input})}|^2 T_{\mathrm{FF}}$ (for simplicity we assume that the barrier is surrounded by air). The final expression for the energy velocity is $V_{\omega,E}=T_{\mathrm{FF}}(L/\tau_\omega)$, where $\tau_\omega=2\int_0^L U_\omega(z)dz/(\varepsilon_0 c|E_\omega^{(\mathrm{input})}|^2)$ is the tunneling time. One may also define a group (or tunneling) velocity associated with the delay of the transmitted pulse as $V_{\omega,g}=L/\tau_\omega$, which leads to the expression $V_{\omega,E}=T_{\mathrm{FF}}V_{\omega,g}$. This expression has been derived with no particular restrictions on the FF beam as it traverses the barrier, and was derived and discussed at length for linear systems in Ref. [11]. It has been experimentally verified in a coaxial photonic crystal [13]. Here we just point out that placing the requirement that energy velocity should remain subluminal ($V_{\omega,E}\leqslant c$) leads directly to the condition $V_{\omega,g}\leqslant c/T_{\mathrm{FF}}$. In the case $T_{\mathrm{FF}}\ll 1$ (as, for example, when the input field is tuned in the gap of the PC) superluminal tunneling velocities are readily accessible [11,14], while in the case $T_{\mathrm{FF}}\gg 1$, as in the present situation, extremely slow tunneling velocities are obtained.

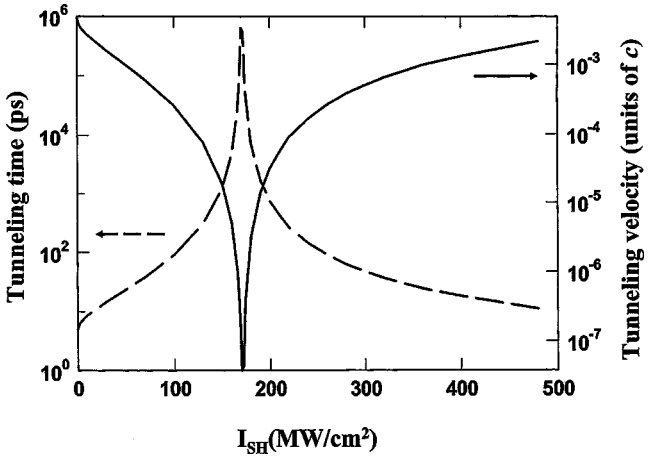

FIG. 4. Tunneling time (dashed line) and tunneling velocity (solid line) of the FF transmitted field vs the SH input intensity for the structure described in Fig. 1.

The expression for $U_\omega(z)$ in the case of two linearly polarized, monochromatic plane waves at FF and SH frequency interacting in a quadratic material with no magnetization is [15]

$$U_\omega(z)=(\varepsilon_0/4)[\mathrm{Re}(\varepsilon_\omega)|E_\omega|^2+(c^2/\omega^2)|dE_\omega/dz|^2 + 2d^{(2)}|E_{2\omega}||E_\omega|^2\cos(\varphi_{2\omega}-2\varphi_\omega)],$$

where ε_ω is the relative dielectric constant, and $\phi_{j\omega}$ are the phases of the fields. From the above expression, we obtain the tunneling time [16]:

$$\tau_\omega=\int_0^L [\mathrm{Re}(\varepsilon_\omega)|E_\omega|^2+(c^2/\omega^2)|dE_\omega/dz|^2 + 2d^{(2)}|E_{2\omega}||E_\omega|^2\cos(\varphi_{2\omega}-2\varphi_\omega)]dz \Big/ (2c|E_\omega^{(\mathrm{input})}|^2).$$

τ_ω is plotted in Fig. 4 as a function of SH input intensity for the structure described in Fig. 1. In the linear regime ($I_{\mathrm{SH}} \rightarrow 0$), we have $\tau_\omega \approx 5$ ps, which corresponds to $V_{\omega,g} \approx c/210$, consistent with the lifetime associated with the bandwidth of the transmission resonance [see inset (b) of Fig. 1]. Increasing the input SH intensity causes a dramatic increase of τ_ω due to the amplification of the FF field: the SH provides approximately six orders of magnitude of gain to the FF, which proves crucial to the tunneling velocity of the FF beam.

When gain inversion occurs ($I_{\mathrm{SH}} \approx 170$ MW/cm^2) the tunneling velocity is $V_{\omega,g} = (L/\tau_\omega) \approx 11$ m/s and $\tau_\omega \approx 630$ ns. Consistent with the picture of equivalence of lifetime and resonance bandwidth, the amplification process thus causes a dynamic, virtual narrowing of the resonance bandwidth by an amount proportional to the net gain, from 5 ps ($\sim 10^3$ GHz) to 630 ns (~ 10 MHz). Therefore, the presence of a SH field inside the structure creates a virtual state for the FF field which consists of a resonance bandwidth of only a few megahertz, resolvable with pulses at least a few microseconds in duration. We note that in the structure of Fig. 3(a) the minimum tunneling velocity of $V_{\omega,g} \approx 11$ m/s is reached for $I_{\mathrm{SH}} \approx 2.7$ GW/cm^2, while for the structure of Fig. 3(b) the same tunneling velocity is reached for $I_{\mathrm{SH}} \approx 5.9$ GW/cm^2.

We have also performed calculations using the geometry described in Fig. 1 and pulses only a few tenths of picoseconds in duration. For amplification factors that do not exceed 10^2, these pulses continue to resolve the resonances well and tunnel the structure approximately undistorted and delayed just as predicted by the tunneling time. Higher gain factors cause picosecond pulses to become compressed in time, distorted, and ultimately break up. Broader virtual resonances that may be resolved with shorter pulses may be created at the expense of increased tunneling velocities. In fact, Fig. 4 suggests that an intensity of $I_{\mathrm{SH}} \approx 160$ MW/cm^2 would create a virtual resonance approximately 1 GHz wide, resolvable with pulses only a few nanoseconds in duration, and yielding a tunneling velocity tunable down to approximately 1000 m/s.

In summary, we have studied a method to achieve and control light confinement using a parametric down-conversion process in a 1D PC. We conclude that extremely small light velocities may more generally be associated, and may be more easily accessible, with any type of resonance phenomenon, with either classical or quantum origins.

This research was supported in part by the U.S. Army and in part by the OPEN Esprit project ANLM.

[1] L. V. Hau *et al.*, Nature (London) **397**, 594 (1999).
[2] M. M. Kash *et al.*, Phys. Rev. Lett. **82**, 5229 (1999).
[3] A. V. Turukhin *et al.*, Phys. Rev. Lett. **88**, 023602 (2002).
[4] G. D'Aguanno *et al.*, Phys. Rev. E **64**, 016609 (2001), and references therein.
[5] Y. Dumeige *et al.*, Phys. Rev. Lett. **89**, 043901 (2002).
[6] G. D'Aguanno *et al.*, J. Opt. Soc. Am. B **19**, 2111 (2002).
[7] G. D'Aguanno *et al.*, Phys. Rev. E **67**, 016606 (2003).
[8] W. H. Press, B. P. Flannery, S. A. Teukolsky, and W. T. Vetterling, *Numerical Recipes in C* (Cambridge University Press, Cambridge, England, 1988).
[9] A. L. Belostotsky, A. S. Leonov, and A. V. Meleshko, Opt. Lett. **19**, 856 (1994).
[10] T. F. Krauss and R. M. De La Rue, Prog. Quantum Electron. **23**, 51 (1999).
[11] G. D'Aguanno *et al.*, Phys. Rev. E **63**, 036610 (2001).
[12] H. G. Winful, Phys. Rev. Lett. **90**, 023901 (2003); Opt. Express **10**, 1491 (2002).
[13] A. Haché and L. Poirer, Appl. Phys. Lett. **80**, 518 (2002).
[14] A. M. Steinberg, P. G. Kwiat, and R. T. Chiao, Phys. Rev. Lett. **71**, 708 (1993).
[15] Y. R. Shen, *The Principles of Nonlinear Optics* (Wiley, New York, 1984).
[16] The SH field remains undepleted, and the maximum value of $d^{(2)}|E_{2\omega}|$ is always less than 10^{-2}. This means that the tunneling time can also be written as $\tau_\omega \cong \int_0^L [\mathrm{Re}(\varepsilon_\omega)|E_\omega|^2 + (c^2/\omega^2)|dE_\omega/dz|^2]dz/(2c|E_\omega^{(\mathrm{input})}|^2)$ with an error always smaller than 1%.